1999

Development of Carbon-Metal Oxide Supercapacitors from Sol-Gel Derived Carbon-Ruthenium Xerogels

Chuan Lin
University of South Carolina - Columbia

James A. Ritter
University of South Carolina - Columbia

Branko N. Popov
University of South Carolina - Columbia, popov@engr.sc.edu

Publication Info

Journal of the Electrochemical Society, 1999, pages 3155-3160.

Journal of The Electrochemical Society, **146** (9) 3155-3160 (1999)
S0013-4651(98)12-085-2 CCC: $7.00 © The Electrochemical Society, Inc.

Development of Carbon-Metal Oxide Supercapacitors from Sol-Gel Derived Carbon-Ruthenium Xerogels

Chuan Lin,[a] James A. Ritter,*,z and Branko N. Popov*

Department of Chemical Engineering, Swearingen Engineering Center, University of South Carolina, Columbia, South Carolina 29208, USA

Sol-gel derived high surface area carbon-ruthenium xerogels were prepared from carbonized resorcinol-formaldehyde resins containing an electrochemically active form of ruthenium oxide. The electrochemical capacitance of these materials increased with an increase in the ruthenium content indicating the presence of pseudocapacitance associated with the ruthenium oxide undergoing reversible faradaic redox reactions. A specific capacitance of 256 F/g (single electrode) was obtained from a carbon xerogel containing 14 wt % Ru, which corresponded to more than 50% utilization of the ruthenium. The double layer accounted for 40% of this capacitance. This material was also electrochemically stable, showing no change in a cyclic voltammogram for over 2000 cycles.

Manuscript submitted December 28, 1998; revised manuscript received May 5, 1999.

There has been increasing interest in electrochemical capacitors[1-5] as energy storage systems because of their high power density and long cycle life, compared to battery devices. According to the mechanism of energy storage, there are two types of electrochemical capacitors. One type is based on double layer (dl) formation due to charge separation, and the other type is based on a faradaic process due to redox reactions. These dl devices are referred to as electrochemical dl capacitors (EDLCs), and faradaic devices are called pseudocapacitors. Depending on the origin of the interaction between the electrode and electrolyte, the associated capacitance is usually in the range of tens (for dl capacitors) to hundreds (for pseudocapacitors) of μF per cm^2 of interfacial area.

Carbon materials, such as activated carbons,[6,7] carbon fibers,[8] and carbon aerogels,[9] are widely used for dl capacitors because of their high surface area. The specific capacitance of these kinds of carbon materials typically ranges from 40 to 160 F/g (single electrode). On the other hand, comparatively lower surface area transition metal oxides, such as amorphous hydrous ruthenium oxide, $RuO_2 \cdot H_2O$, [10] have been studied for pseudocapacitors. A remarkable specific capacitance of 760 F/g (single electrode) was achieved for this material made by the sol-gel technique. Moreover, a recent modeling study has shown that electrode materials possessing both double layer and reversible redox processes can enhance the energy density of a device.[11]

The dl mechanism of energy storage is strictly a surface phenomenon, with higher active surface areas giving rise to higher specific capacitances. In contrast, the faradaic mechanism of energy storage is not limited to surface reactions; bulk reactions are also possible and contribute to energy storage in these kinds of materials.[10] However, proton diffusion into the bulk of the material, an inherently slow transport mechanism, would likely limit the power of such a device and thus the utilization of the material. It would be advantageous to disperse a relatively low surface area, redox-active transition metal oxide such as $RuO_2 \cdot xH_2O$ throughout a high surface area, double layer support such as activated carbon. The resulting small particle size of the $RuO_2 \cdot xH_2O$ would increase the redox-active surface area of the material, giving rise to higher-power devices and more utilization of this expensive transition metal oxide. The sol-gel technique is well suited for making this kind of material, because it readily allows for control of the texture, composition, homogeneity, and structural properties of the resulting materials.[12] Recently, Miller *et al.* prepared an electrode material for supercapacitors, with ruthenium nanoparticles deposited via chemical vapor deposition within the pore of a carbon aerogel.[13] They achieved a specific capacitance of 206 F/g (single electrode) for an areogel containing 35 wt % ruthenium.

The objective of this work is to present an alternative method for making high surface area carbon-ruthenium xerogel composites for use as supercapacitors. This new method is based on a sol-gel route for making high surface area carbon xerogels from carbonized resorcinol-formaldehyde (R-F) resins.[14] Physical properties of these unique xerogel composites, such as surface area, pore volume, crystallinity, and surface morphology, are reported along with their performance as electrochemical capacitors utilizing both dl and faradaic processes.

Experimental

The synthesis procedure presented below for making carbon-ruthenium xerogels was based on similar procedures that have been used for making carbon aerogels[9] and carbon xerogels.[14] Reagent-grade resorcinol (98%, Aldrich), formaldehyde (37% in water, Aldrich), sodium carbonate (GR, EM Science, Germany), acetone (ACS, 99.5%, Alfa), and $RuO_2 \cdot xH_2O$ (Ru 55.29%, Alfa) were used as received. Briefly, solutions containing 20 wt/vol % solids were prepared, in which the R-F mole ratio (R/F) was fixed at 1:2. Sodium carbonate was used as a catalyst and the resorcinol/sodium carbonate mole ratio (R/C) was fixed at 50. The $RuO_2 \cdot xH_2O$/resorcinol mole ratio (Ru/R) was varied to make carbon-ruthenium xerogels with different Ru loadings. $RuO_2 \cdot xH_2O$ was added as a powder prior to the partial polymerization of R-F to a sol state, and its addition slightly decreased the pH of the initial R-F solution from 7.5 (Ru/R = 0) to 6.9 (Ru/R = 0.1). The solutions were sealed in a glass bottle and magnetically stirred at room temperature until gelation occurred, and then the gels were placed in an oven (85 $\pm$ 3°C) for curing for 1 week. The resultant gels were opaque instead of the characteristic deep red color of unmodified R-F gels.[9] After curing, the gels were washed with acetone for three days. Fresh solvent was replaced daily after vacuum filtration. Then the washed gels were dried under N_2 in a tube furnace. Using a heating rate of 0.5°C/min, the furnace was heated to 65°C and held at that temperature for 5 h; it was then heated to 110°C and held there for another 5 h. Finally, the carbon-ruthenium xerogels were formed by pyrolysis of the dried gels at 750°C in a N_2 atmosphere for 3 h with both heating and cooling rates set at 5°C/min.

The surface areas and pore volumes of the carbon-ruthenium xerogels were measured using a Micromeritics Pulse Chemisorb 2700 analyzer. Transmission electron micrographs were recorded with a Hitachi H-8000 transmission electron microscope (TEM), and X-ray diffraction (XRD) patterns were collected using a Rigaku-D-max B diffractometer equipped with a Cu source. Electrochemical

* Electrochemical Society Active Member.
[a] Present Address: Department of Chemical Engineering, Center for Advanced Engineering Fibers and Films, Clemson University, Clemson, South Carolina 29634, USA.
[z] E-mail: ritter@engr.sc.edu.

S0013-4651(98)12-085-2 CCC: $7.00 © The Electrochemical Society, Inc.

measurements were carried out at room temperature using an EG&G 273A potentiostat.

A three-electrode test system was used to make the electrochemical measurements. The working electrode, containing about 1 to 2 mg of active material and 5 wt % Teflon as binder, was hand-pressed into a disk with a diameter of 0.75 cm and thickness of about 50 μm. The disk was then pressed between two pieces of platinum gauze at 3 tons/cm^2 with a hydraulic press and held there for 10 min. A saturated calomel electrode (SCE) was used as the reference electrode, a piece of platinum gauze (large, relative to the working electrode) was used as the counter electrode, and a solution of 30 wt % H_2SO_4 was used as the electrolyte. Galvanostatic charge/discharge was performed between 0 and 1 V (*vs.* SCE) by varying the current density (0.1 to 50 mA/mg), and cyclic voltammetry (CV) was carried out between 0 and 1 V (*vs.* SCE) with a sweep rate of 5 mV/s. The electrochemical measurements were conducted at room temperature.

The specific capacitances of the single electrode were calculated from the galvanostatic discharge using the following equation

$$C = \frac{it_d}{m\Delta V_{CC}} \quad [1]$$

where C is the specific capacitance, i is the total current, t_d is the discharge time, ΔV_{CC} is the potential drop during constant current discharge, and m is the mass of the active material. For comparison, the specific capacitances were also calculated from the cathodic part of the CV results using the following equation

$$C = \frac{1}{m\Delta V_{CV}} \int_1^2 i_c dt \quad [2]$$

where i_c is the cathodic current, t is the time, t_1 is the time when V = 0.9 V, t_2 is the time when V = 0.1 V, and ΔV_{CV} is the potential difference (0.8 V). The specific energy and power of the single electrode were also calculated from the galvanostatic discharge results using the following equations

$$\text{Specific energy} = \frac{i\overline{V}t_d}{m} \quad [3]$$

$$\text{Specific power} = \frac{i\overline{V}}{m} \quad [4]$$

where the average potential, $\overline{V}$, is given by

$$\overline{V} = \frac{1}{t_d} \int_0^{t_d} V dt \quad [5]$$

Results

Different carbon-ruthenium xerogels were made by varying the Ru/R mole ratio in the initial R-F solution between 0 and 0.1 (Ru/R = 0.1 is equivalent to 14 wt % Ru in the resultant carbon-ruthenium xerogel). It is noteworthy that gelation did not occur above Ru/R = 0.1. Figure 1 shows the effect of the Ru content on the surface area and pore volume of the carbon-ruthenium xerogels. The surface area was 563 m^2/g for the pure carbon xerogel (Ru/R = 0). It then dropped sharply to 520 m^2/g with an increase of Ru/R from 0 to 0.01. With an increase of Ru/R up to 0.1, the surface area decreased more slowly and almost linearly to 475 m^2/g. In contrast, the pore volume increased significantly and linearly from 0.23 to 0.59 cm^3/g with an increase of Ru/R from 0 to 0.1.

The effect of Ru content on the crystalline structure of fresh carbon-ruthenium xerogels is shown in Fig. 2A. The XRD patterns for the pure carbon xerogel exhibited two broad humps at 2θ = 22 and 43°, which corresponded to a typical microcrystalline carbon structure. As the Ru content increased, however, the carbon humps decreased gradually and almost disappeared for the carbon-ruthenium xerogel with Ru/R = 0.1. The XRD patterns for the carbon-ruthenium xerogels also showed characteristic peaks of Ru metal at 2θ = 38.4, 42.2, 44.0, 58.3, and 69.5°, and the intensities of these peaks increased with increasing Ru content. Figure 2B displays

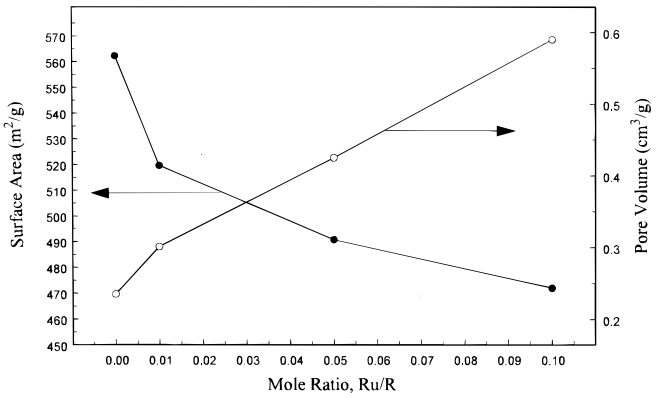

Figure 1. Effect of Ru content on the surface area and pore volume of the carbon-ruthenium xerogels.

XRD patterns for different Ru materials. The as-received $RuO_2 \cdot xH_2O$, which was used for making the carbon-ruthenium xerogels in the initial solution, was essentially amorphous. For the carbon-ruthenium xerogel with Ru/R = 0.1, the XRD patterns for fresh xerogel, and that after 2000 CV cycles, both exhibited peaks that are characteristic of Ru metal, but the intensities of the peaks decreased by about 80% after CV cycling. In addition, the XRD pattern of RuO_2, which was made by calcining the as-received $RuO_2 \cdot xH_2O$ at

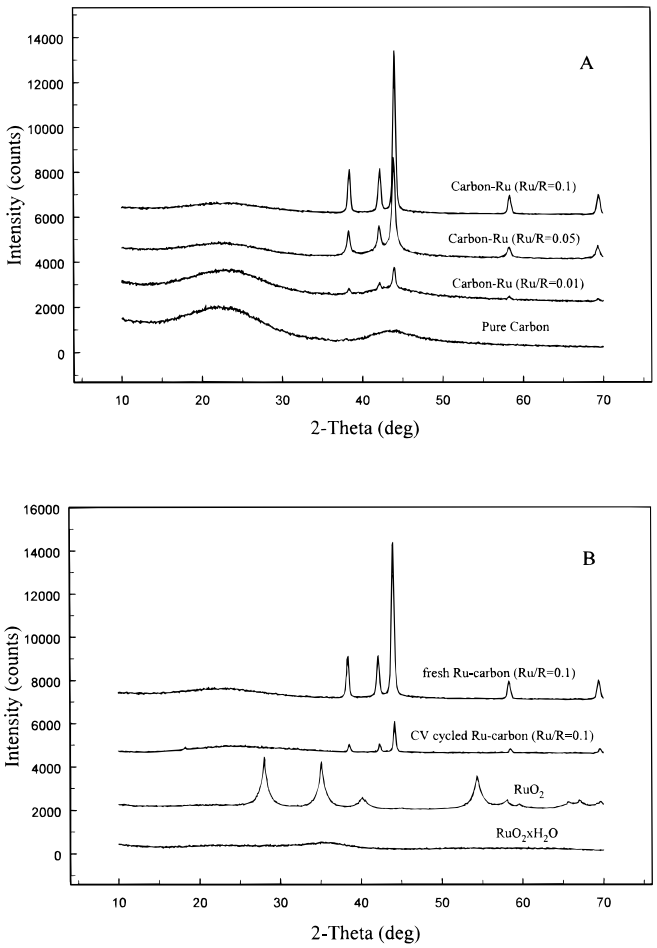

Figure 2. (A) XRD patterns of carbon-ruthenium xerogels with different Ru loadings; and (B) comparison of XRD patterns of carbon-ruthenium xerogels (Ru/R = 0.1) before and after 2000 CV cycles, as-received $RuO_2 \cdot xH_2O$, and RuO_2 (*i.e.*, calcined $RuO_2 \cdot xH_2O$ at 400°C in air for 3 h).

S0013-4651(98)12-085-2 CCC: $7.00 © The Electrochemical Society, Inc.

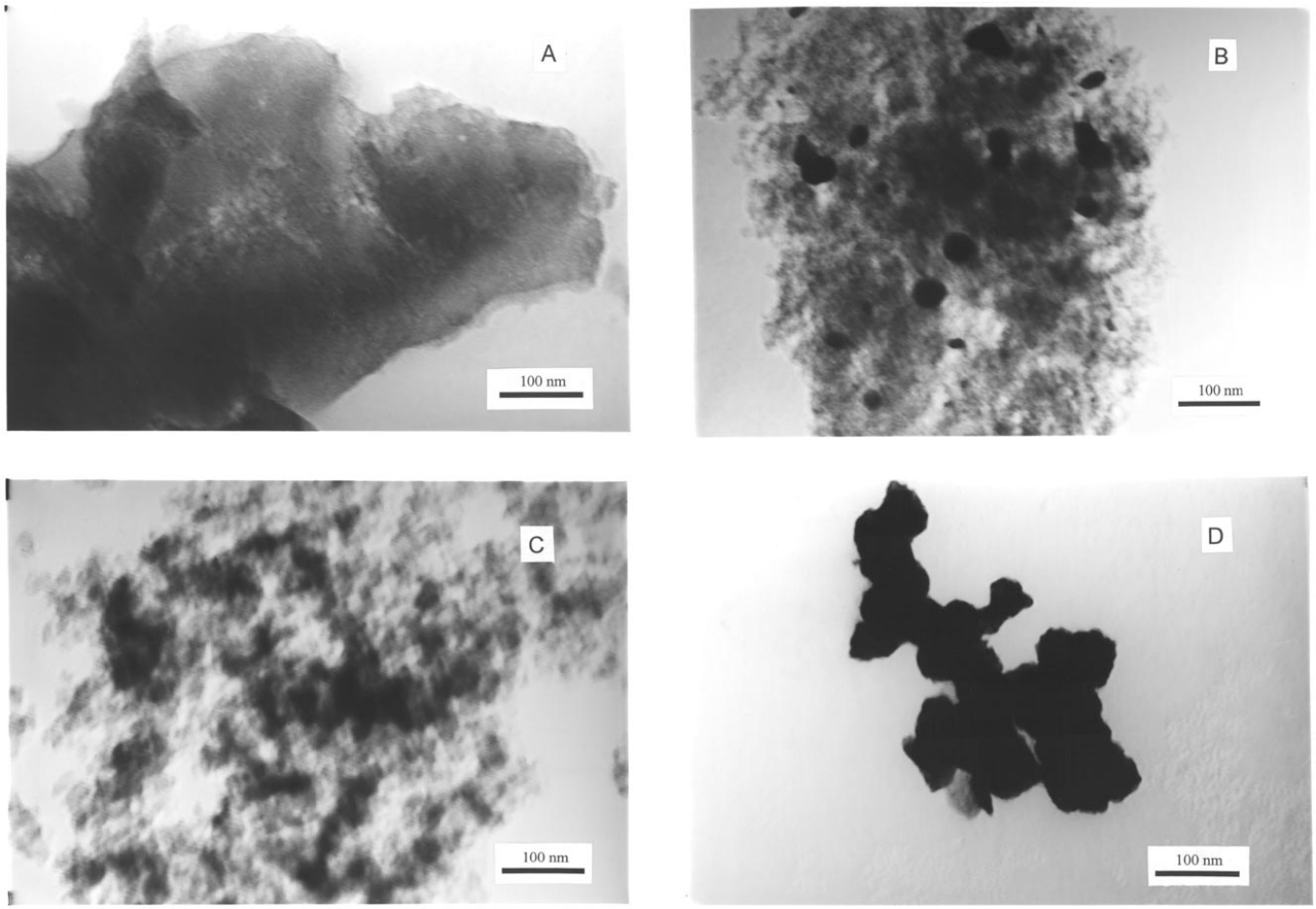

Figure 3. TEM images: (A) pure carbon xerogel; (B) carbon-Ru xerogel with Ru/R = 0.01; (C) carbon-Ru xerogel with Ru/R = 0.1; and (D) as-received $RuO_2 \cdot xH_2O$.

400°C in air for 3 h, indicated that both the fresh and CV cycled carbon-ruthenium xerogels did not contain any crystalline RuO_2.

The surface morphology of the carbon-ruthenium xerogels was studied with TEM; the TEM micrographs are shown in Fig. 3A to C. The pure carbon xerogel (Fig. 3A) exhibited a very fine pore structure. In contrast, the xerogel with Ru/R = 0.01 (Fig. 3B) had black spots dispersed randomly in the carbon matrix that ranged from 10 to 30 nm in diam. These spots were identified as metallic Ru nanoparticles. The xerogel with Ru/R = 0.1 (Fig. 3C), as expected, showed a higher population of ruthenium particles with sizes similar to those in Fig. 3B. For comparison, a TEM micrograph of the as-received $RuO_2 \cdot xH_2O$ is shown in Fig. 3D; particle sizes for this material ranged from 50 to 100 nm in diam.

CV and galvanostatic techniques were used to determine the electrochemical properties of the carbon-ruthenium xerogels and also the as-received $RuO_2 \cdot xH_2O$. Figure 4A shows CVs of the car-

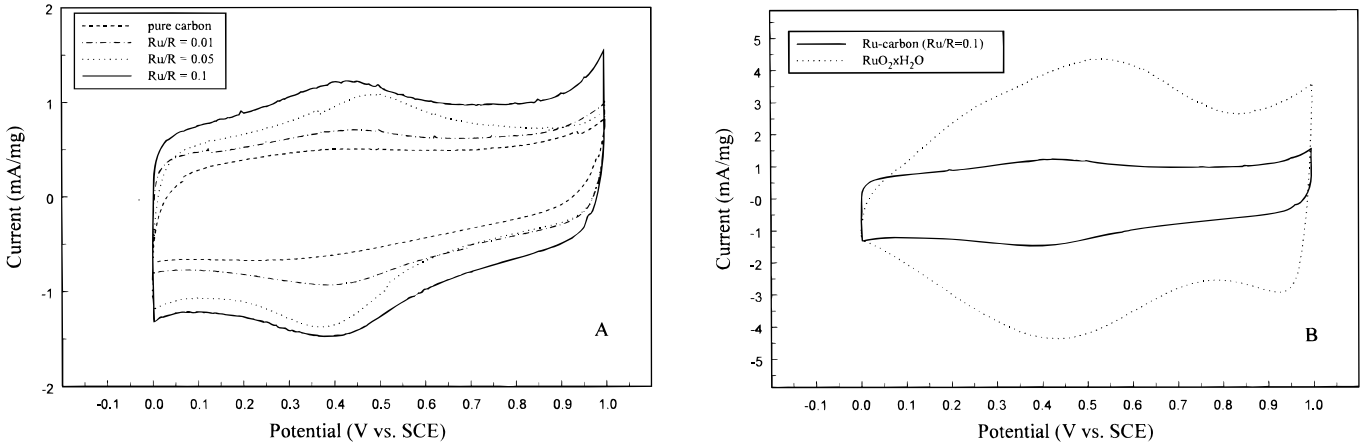

Figure 4. CVs of Ru-carbon xerogels with different Ru loadings; and (B) comparison of CVs for the carbon-ruthenium xerogel with Ru/R = 0.1 and as-received $RuO_2 \cdot xH_2O$. In all cases, the scan rate was 5 mV/s.

S0013-4651(98)12-085-2 CCC: $7.00 © The Electrochemical Society, Inc.

bon-ruthenium xerogels as a function of the Ru content. The constant current observed with variation in potential was characteristic of capacitive behavior. The CV curve also exhibited ideal pseudocapacitive behavior between the hydrogen and oxygen evolution reactions. The current increased with an increase in the Ru content, indicating a higher capacitance for xerogels with a higher Ru content. Figure 4B presents CVs for the carbon-ruthenium xerogel with Ru/R = 0.1 and the as-received $RuO_2 \cdot xH_2O$. The as-received $RuO_2 \cdot xH_2O$ had a much higher capacitance than the carbon-ruthenium xerogel. In addition, the shapes of their respective voltammograms were different. The carbon-ruthenium xerogel behaved more like a capacitor material and exhibited a relatively flat current response over a broad potential range. In contrast, $RuO_2 \cdot xH_2O$ behaved more like a redox material with distinguishable broad peaks. The electrochemical stability of the carbon-ruthenium xerogel with Ru/R = 0.1 was studied using CV; the results are shown in Fig. 5. Essentially, no change was observed between the initial cycle and after 2000 cycles, indicating that the electrode was very stable and that much of the Ru metal in the carbonized material was converted to an electrochemically active form during the first cycle.

Figure 6A shows constant-current discharge profiles of the carbon-ruthenium xerogels at a current density of 1 mA/mg. The profiles were similarly shaped for all of the carbon-ruthenium xerogels; however, the discharge time for the potential change from 1 to 0 V increased with an increase in Ru content, indicating that the capacitance increased with increasing Ru content. The initial potential drops observed in Fig. 6A were caused by non-uniform current distributions as a result of ohmic and pore resistances.[11,15] Figure 6B presents constant-current discharge profiles of the carbon-ruthenium xerogel with Ru/R = 0.1 and the as-received $RuO_2 \cdot xH_2O$, both at a current density of 1 mA/mg. The corresponding capacitances were 232 and 675 F/g, respectively. It was interesting that the essentially faradaic electrode ($RuO_2 \cdot xH_2O$) did not exhibit the initial drop in potential, which was more characteristic of a battery discharged at high current densities. Figure 7 shows the effect of Ru content on the capacitance of the carbon-ruthenium xerogels, measured by constant-current discharge at a current density of 1 mA/mg and by CV at a sweep rate of 5 mV/s. As shown in Fig. 7, the capacitance obtained by constant-current discharge was always about 10 to 15% higher than that obtained by CV. Because the transition discharge time was easier to determine and thus more accurate than the total cathodic or anodic charge from the CV, any capacitance referred to below is based on the constant-current discharge method unless stated otherwise. The capacitance was about 120 F/g for pure carbon xerogel, and it increased with an increase in Ru content and reached 232 F/g for the xerogel with Ru/R = 0.1.

During galvanostatic experiments, the capacitance of the carbon-ruthenium xerogels also varied with current density. The results for the carbon-ruthenium xerogel with Ru/R = 0.1 and the pure carbon xerogel are shown in Fig. 8A. The capacitance decreased almost linearly with an increase in the log of the current density in both cases. For the carbon-ruthenium xerogel, a capacitance as high as 256 F/g was obtained at a current density of 0.1 mA/mg; however, it dropped

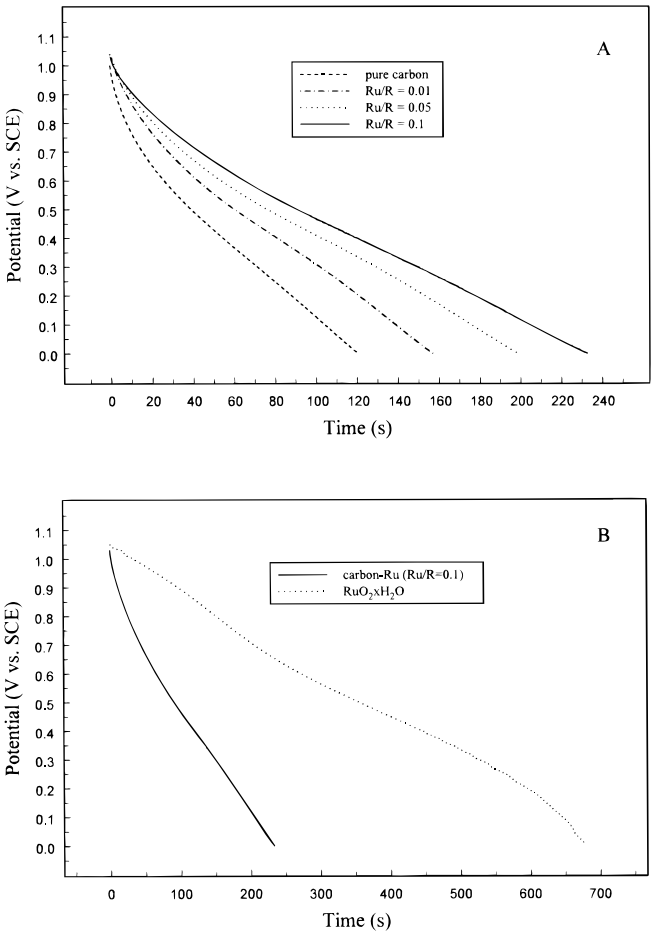

Figure 6. (A) Constant current discharge profiles of carbon-ruthenium xerogels with different Ru loadings; and (B) comparison of constant current discharge profiles for the carbon-ruthenium xerogel with Ru/R = 0.1 and as-received $RuO_2 \cdot xH_2O$. In all cases, the current density was 1 mA/mg.

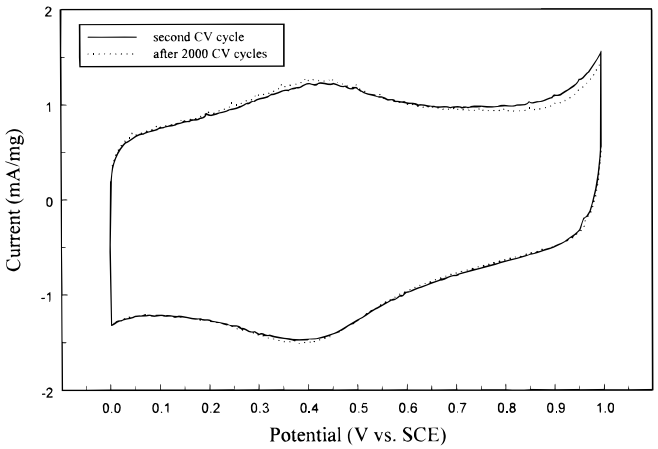

Figure 5. Stability of the carbon-ruthenium xerogel with Ru/R = 0.1, measured at a scan rate of 5 mV/s.

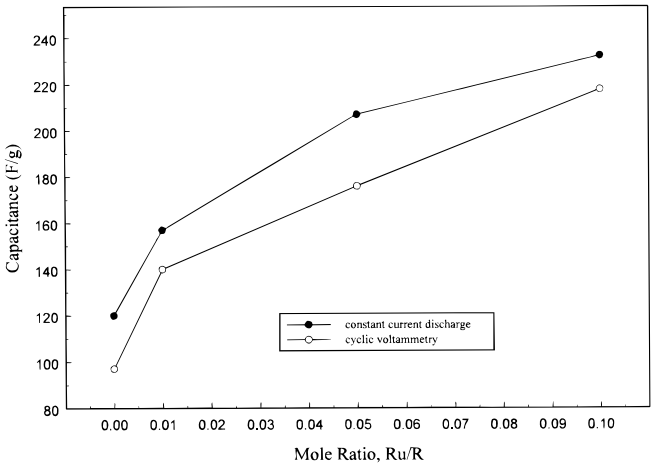

Figure 7. Effect of Ru content on the capacitance of the carbon-ruthenium xerogels, measured by constant current discharge at a current density of 1 mA/mg and by CV at a sweep rate of 5 mV/s.

S0013-4651(98)12-085-2 CCC: $7.00 © The Electrochemical Society, Inc.

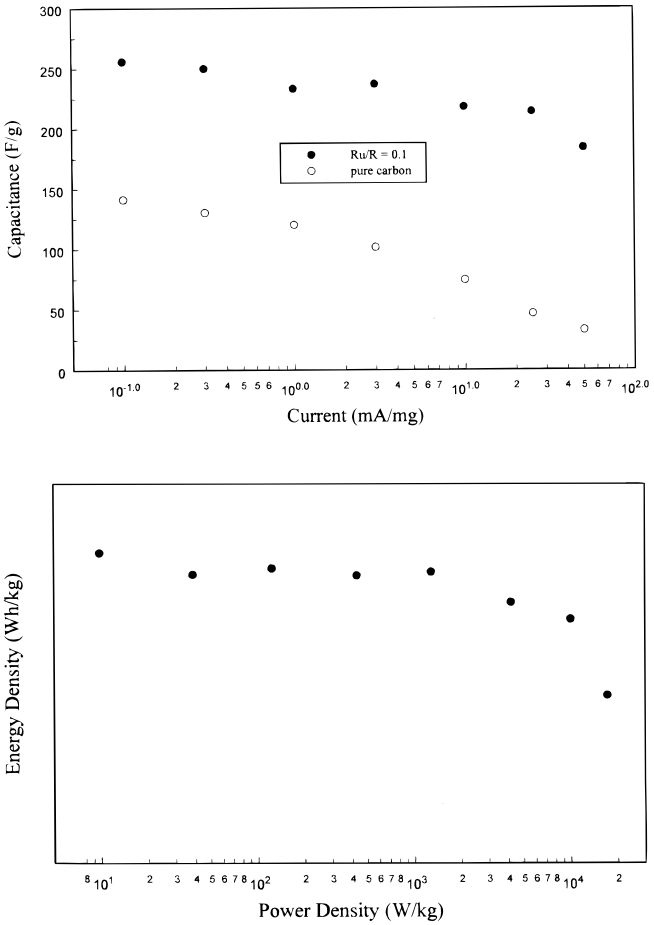

Figure 8. (A) Effect of current density on the capacitance of the carbon-ruthenium xerogel with Ru/R=0.1 and the pure carbon xerogel; and (B) Ragone plot for the single electrode containing the carbon-ruthenium xerogel with Ru/R = 0.1.

to about 184 F/g at a current density of 50 mA/mg. For the pure carbon xerogel, the capacitances were 142 and 34 F/g at current densities of 0.1 and 50 mA/mg, respectively. A Ragone plot for the single electrode containing the carbon-ruthenium xerogel with Ru/R = 0.1 is presented in Fig. 8B. The energy density remained constant at about 30 Wh/kg up to a power density of 1000 W/kg, then the energy density began to drop off at higher power densities. It is noteworthy that these are average power densities, not peak power densities; and that the per kilogram basis includes only the mass of the electrode material.

Discussion

High surface area carbon-ruthenium xerogels were made with the sol-gel technique, and their pore structure was measured in terms of surface area and total pore volume (Fig. 1). The surface area of the carbon-ruthenium xerogels decreased with an increase in Ru content; however, the pore volume increased with an increase in Ru content. A decreasing surface area with an increasing pore volume is indicative of the presense of larger pores with an increase in Ru content, which implies less shrinkage of the gel structure with an increase in Ru content. Less shrinkage of the gel structure may have also been caused by the slight decrease in pH of the initial R-F solution that occurred after addition of the $RuO_2 \cdot xH_2O$. This decrease in pH may have enhanced the condensation reaction[14] of the R-F system, thereby leading to a more cross-linked R-F resin and hence, larger pores.

The XRD patterns in Fig. 2A revealed that the ruthenium in the carbon xerogels was in the form of metal dispersed throughout the carbon matrix, even though it was added as an oxide ($RuO_2 \cdot xH_2O$) to the initial R-F solution. The ruthenium metal likely formed during carbonization according to the following reaction, because carbon is a good reductant at high temperatures

$$RuO_2 \cdot xH_2O + 2C = Ru + 2CO + xH_2O \qquad [6]$$

Nevertheless, after one charge/discharge cycle, the majority of the ruthenium metal inside the carbon matrix was converted into a hydrous oxide form similar to the as-received $RuO_2 \cdot xH_2O$. This hydrous oxide was electrochemically active and gave rise to the higher capacitances observed with the carbon xerogels containing ruthenium as shown in Fig. 7. This explanation is consistent with the XRD patterns shown in Fig. 2B. Birss *et al.*[16] studied the formation of oxide films on Ru metal electrodes. They found that after charge/discharge between 0 and 1.4 V (*vs.* saturated hydrogen electrode, SHE), a hydrous ruthenium oxide film formed on the Ru metal surface and its thickness increased with cycling. This oxide film was also not reducible to metal in the positive potential range. The results presented here are consistent with their finding[16] in that the Ru metal nanoparticles were converted to a very stable form of hydrous ruthenium oxide after charge/discharge.

The TEM results indicated that the ruthenium particles in the carbon-ruthenium xerogels, ranging between 10 and 30 nm, were smaller than those in the as-received $RuO_2 \cdot xH_2O$, which ranged between 50 and 100 nm (Fig. 3). There are two plausible reasons for this difference. First, Fig. 3D shows that the $RuO_2 \cdot xH_2O$ particles were comprised of aggregates of smaller particles in the range of 30 to 70 nm. These aggregates most likely broke up into individual particles in the initial R-F solution, especially because $RuO_2 \cdot xH_2O$ is slightly soluble in aqueous solutions. Second, the ruthenium particles in the carbon xerogels were metallic and formed according to Eq. 6. These consecutive events of aggregate breakup, followed by dispersion in the carbon matrix and subsequent dehydration and reduction to ruthenium metal likely gave rise to the smaller metallic ruthenium nanoparticles of about 10 to 30 nm in diam. These metallic particles also converted into an electrochemically active form after CV cycling, as explained above. Note that the particle size after cycling was not investigated, because it was very difficult to recover the active electrode material from the cell after cycling.

The electrochemical studies also showed that these carbon-ruthenium xerogels utilized both the dl capacitance associated with the high surface area carbon xerogel and the pseudocapacitance associated with the ruthenium redox reactions. For example, the capacitance increased with an increase in Ru content (Fig. 7) from 120 F/g for the pure carbon to 232 F/g for the xerogel with Ru/R = 0.1. This result was clearly due to the pseudocapacitance associated with the ruthenium inside the carbon matrix. The results in Fig. 8 show that at a current density of 0.1 mA/mg, the capacitances were 256 and 142 F/g for the carbon-ruthenium xerogel with Ru/R = 0.1 and pure carbon xerogel, respectively. Becasue there was 0.14 g of Ru in 1 g of the carbon-ruthenium xerogel (*i.e.*, with Ru/R = 0.1), the capacitance from the ruthenium redox reaction was approximately 956 F/g of Ru after subtracting the carbon contribution, based on the ruthenium-free carbon xerogel (*i.e.*, with Ru/R = 0.0). Also, assuming a two-electron transfer for Eq. 7, the theoretical capacitance for the ruthenium redox reaction was 1907 F/g of Ru. Therefore, the ruthenium utilization was about 50% for the carbon-ruthenium xerogel with Ru/R = 0.1 at a current density of 0.1 mA/mg. Actually, the ruthenium utilization was probably somewhat higher than 50% because δ was actually a little less than 2, and also according to the surface area and pore volume results. The surface area and pore volume decreased and increased, respectively, with an increase in Ru content (Fig. 1). Therefore, the dl capacitance alone probably decreased slightly compared to the pure carbon xerogel, which suggests even more electrochemical activity for the ruthenium inside the carbon matrix.

The charge storage mechanism for the reversible ruthenium redox reaction has been explained in terms of a proton-electron reaction mechanism in which ruthenium oxide and $RuO_2 \cdot xH_2O$ can be reduced and oxidized reversibly through electrochemical protonation[17,18]

S0013-4651(98)12-085-2 CCC: $7.00 © The Electrochemical Society, Inc.

$$RuO_2 + \delta H^+ + \delta e^- \leftrightarrow RuO_{2-\delta}(OH)_\delta \quad 0 \leq \delta \leq 2 \qquad [7]$$

This reversible redox reaction gives rise to the broad anodic and cathodic peaks in the CV curves for the samples containing ruthenium, as shown in Fig. 4. The ruthenium valence state changes from $Ru^{2+}(OH)_2$ at about 0 V (*vs.* SHE) to $Ru^{4+}O_2$ at about 1.4 V (*vs.* SHE) upon complete oxidation, with proton diffusion within the bulk of the material being the rate-determining step for the faradaic reaction. In this study, the maximum charge potential was up to 1 V (*vs.* SCE), which is 0.16 V lower than 1.4 V (*vs.* SHE). As a result, no crystalline ruthenium oxide formed during charge/discharge and again, δ was probably less than 2.

Figure 8A also shows that carbon-ruthenium xerogel with Ru/R = 0.1 consistently exhibited a much higher capacitance over a very broad range of currents compared to the pure carbon xerogel. The decrease in the capacitance that was exhibited by both materials with increased current was also less pronounced for the carbon-ruthenium xerogel with Ru/R = 0.1. This last result is also reflected in Fig. 8B, which shows that the carbon-ruthenium xerogel with Ru/R = 0.1 maintained an energy density of approximately 30 Wh/kg up to a power density of 1000 W/kg. The capacitance of a pure carbon xerogel is linked directly to its specific surface area. However, increasing the surface area above that corresponding to the formation of micropores less than about 0.5 nm in diam does not necessarily result in a corresponding increase in capacitance, because pores in this size range remain inaccessible to the electrolyte and thus do not form a dl.[19] Consequently, there is a limit to the energy and power densities that can be obtained from any carbonaceous materials. As shown in Fig. 8A and B, however, it is possible to further increase the energy density of a material, beyond that which is possible based solely on a dl mechanism, by utilizing a faradaically active material such as $RuO_2 \cdot xH_2O$. Thus, the clear advantage of this kind of carbon-ruthenium xerogel material is that it utilizes both the faradaic capacitance of the metal oxide and the dl capacitance of the carbon. Also, the results in Fig. 8 tend to suggest that the ability of the carbon-ruthenium xerogel with Ru/R = 0.1 to sustain a high energy density over a broad range of power density is due to the faradaic contributions arising from the ruthenium. Similar trends have been reported recently based on a modeling study of a capacitor with dl and faradaic processes.[11]

Conclusions

Sol-gel derived high surface area carbon-ruthenium xerogels were prepared from R-F resins containing $RuO_2 \cdot xH_2O$. Carbonization at 750°C in nitrogen converted the resin into a conductive carbon xerogel and the $RuO_2 \cdot xH_2O$ into metallic ruthenium particles 10 to 30 nm in diam that were subsequently oxidized to an electrochemically active form of ruthenium oxide after one charge/discharge cycle. A very high specific capacitance of 256 F/g (single electrode) was obtained from a carbon xerogel containing 14 wt % Ru. This corresponded to utilizing more than 50% of the ruthenium. Moreover, about 40% of the capacitance was attributed to the formation of a dl within the pores of the high surface area carbon xerogel support during charge/discharge, and about 60% of the capacitance was attributed to the ruthenium oxide dispersed throughout the carbon xerogel matrix undergoing reversible redox reactions during charge/discharge. This material also showed no change in electrochemical capacitance after 2000 charge/discharge cycles, indicating that the material was very stable and the redox reactions associated with the ruthenium oxide were completely reversible.

Acknowledgments

This material is based upon work supported in part by the U.S. Army Research Office under grant no. DAAH04-96-1-0421 and in part by the U.S. Department of Energy under Cooperative Agreement no. DE-FC02-91ER75666.

University of South Carolina assisted in meeting the publication costs of this article.

References

1. B. E. Conway, *J. Electrochem. Soc.*, **138** , 1539 (1991).
2. I. D. Raistrick, in *Electrochemistry of Semiconductors and Electrodes*, J. McHardy and F. Ludwig, Editors, pp. 297-355, Noyes Publications, Park Ridge, NJ (1992).
3. B. E. Conway, in *Third International Seminar on Double Layer Capacitors and Similar Energy Storage Devices*, Boca Raton, FL (1993).
4. S. Trasatti and P. Kurzweil, *Platinum Met. Rev.*, **38,** 46 (1994).
5. S. Sarangapani, B. V. Tilak, and C.-P. Chen, *J. Electrochem. Soc.*, **143,** 3791 (1996).
6. M. Aoki, K. Sato, and Y. Kobayashi, *IEICE Trans. Fundamentals Electronics, Communications, and Computer Sciences*, **E77-A,** 208 (1994).
7. H. Shi, *Electrochim. Acta*, **41,** 1633 (1996).
8. I. Tanahashi, A. Yoshida, and A. Nishino, *Carbon*, **29,** 1033 (1991).
9. S. T. Mayer, R. W. Pekala, and J. L. Kaschmitter, *J. Electrochem. Soc.*, **140,** 446 (1993).
10. J. P. Zheng, P. J. Cygan, and T. R. Jow, *J. Electrochem. Soc.*, **142,** 2699 (1995).
11. C. Lin, J. A. Ritter, B. N. Popov, and R. E. White, *J. Electrochem. Soc.*, **146**, 3168 (1999).
12. C. J. Brinker and G. W. Scherer, *Sol-Gel Science*, Academic Press, San Diego, CA (1990).
13. J. M. Miller, B. Dunn, T. D. Tran, and R. W. Pekala, *J. Electrochem. Soc.*, **144,** L309 (1997).
14. C. Lin and J. A. Ritter, *Carbon*, **35,** 1271 (1997).
15. V. Srinivasan and J. W. Weidner, *J. Electrochem. Soc.*, **146,** 1650 (1999).
16. V. Birss, R. Myers, H. Angerstein-Kozlowska, and B. E. Conway, *J. Electrochem. Soc.*, **131,** 1502 (1984).
17. D. Michell, D. A. J. Rand, and R. Woods, *J. Electroanal. Chem.*, **89,** 11 (1978).
18. S. Trasatti and G. Lodi, in *Electrodes of Conductive Metallic Oxides-Part A*, S. Trasatti, Editor, p. 301, Elsevier, New York (1980).
19. C. Lin, J. A. Ritter, and B. N. Popov, *J. Electrochem. Soc.*, Accepted for publication.